View metadata, citation and similar papers at core.ac.uk

brought to you by CORE

provided by Purdue E-Pubs

Purdue University
Purdue e-Pubs

Birck and NCN Publications | Birck Nanotechnology Center

4-1-2012

A non-obtrusive technique to characterize dielectric charging in RF-MEMS capacitive switches

Sambit Palit
Purdue University, spalit@purdue.edu

Ankit Jain
Purdue University, jain28@purdue.edu

Muhammad A. Alam
Purdue University

Follow this and additional works at: http://docs.lib.purdue.edu/nanopub

Part of the Electro-Mechanical Systems Commons, and the Nanoscience and Nanotechnology Commons

Palit, Sambit; Jain, Ankit; and Alam, Muhammad A., "A non-obtrusive technique to characterize dielectric charging in RF-MEMS capacitive switches" (2012). *Birck and NCN Publications.* Paper 917.
http://docs.lib.purdue.edu/nanopub/917

This document has been made available through Purdue e-Pubs, a service of the Purdue University Libraries. Please contact epubs@purdue.edu for additional information.

A non-obtrusive technique to characterize dielectric charging in RF-MEMS capacitive switches

Sambit Palit[+], Ankit Jain and Muhammad A Alam*
School of Electrical & Computer Engineering, Purdue University
West Lafayette, IN 47906, USA
Phone : 765-494-5988, Email : [+]spalit@purdue.edu, *alam@purdue.edu

***Abstract* – Degradation and failure due to dielectric charging has been a dominant and pervasive reliability concern for RF-MEMS switches. Traditionally, the operational lifetime dictated by this degradation phenomenon is extrapolated from a series of measurements of time-dependent shifts in Capacitance-Voltage (C-V) characteristics under accelerated stress conditions. In this paper, we explain why the classical large-signal C-V methodology may lead to a pessimistic under-prediction of device lifetime. Using both simulations and experiments, we propose and verify a new small-signal characterization technique based on resonance characteristics of MEMS cantilever beams. This new technique overcomes the limitations of the classical approaches to accurately anticipate device lifetime and opens up the possibility of non-obtrusive, in-situ runtime monitoring of degradation in RF-MEMS switches. Moreover, since the technique is amenable to 'parallel' implementation, it has the potential to be used both as an in-line process monitor as well as to reduce the overall time to technology qualification.**

Keywords – RF-MEMS; dielectric films; reliability; modeling; characterization technique; resonance; charge trapping.

I. INTRODUCTION

Radio-Frequency Micro-Electro Mechanical Systems (RF-MEMS) can potentially be used in a wide range of applications like accelerometers, pressure-sensors, RF-switches and tunable capacitors [1]. Fig. 1a shows a typical RF-MEMS switch configuration based on a cantilever beam. A schematic representation in Fig. 1b shows how the beam is separated from the drain (D) electrode by a dielectric and an air-gap. The cantilever is actuated by the electrostatic pull of the control gate (G). This switch in Fig. 1 will be used as a test-bed for the ideas discussed in this paper. Although the commercial RF-MEMS switches involve more complex beam design and different electrode configurations [2] (fixed-fixed or crab-leg beams, ohmic or capacitive switches) to improve performance and simplify integration, the techniques developed in this paper are general and will apply to all RF-MEMS switches or NEMFET (Nano-Electro Mechanical Field Effect Transistor) devices.

Generally speaking, a RF-MEMS switch operates between two bi-stable states of the beam, controlled by an externally applied potential at the control gate (G) (see Fig. 1). In the UP or pulled-out (PO) state, the applied voltage is low and the beam is suspended above the substrate, and separated by the dielectric and an air-gap. Therefore the PO state is characterized by low capacitance and/or low conductivity between the membrane and the substrate contacts. In the DOWN or pulled-in (PI) state, the electrostatic force due to a high external potential at the control gate overcomes the elastic restoring force of the cantilever and pulls the beam down. Since the air-gap is no longer present, the PI state is thus characterized by high capacitance and/or high conductivity between the membrane and the substrate contacts. This difference in the electronic properties of the two states finds applications in signal routing, impedance matching networks and adjustable gain amplifiers.

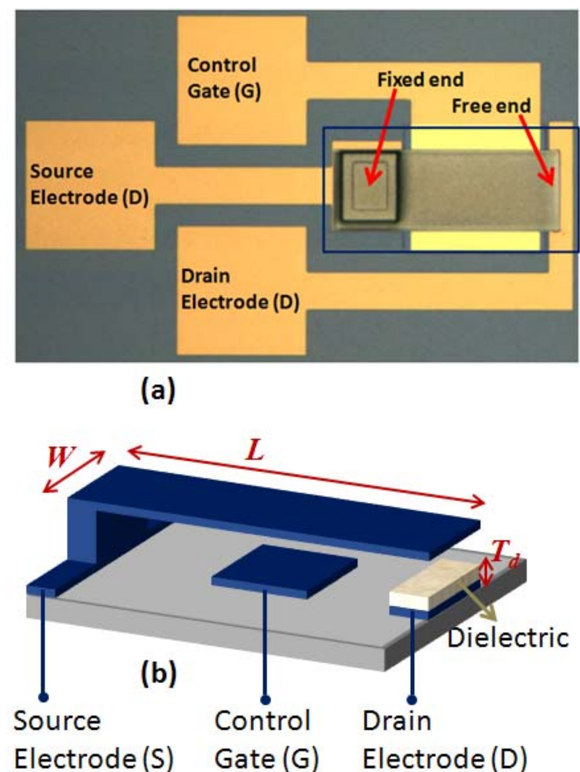

Figure 1: **(a)** Image of a typical cantilever RF-MEMS switch with three electrical terminals (Source: S, Drain: D and Gate: G) as marked. **(b)** A schematic diagram of the cantilever RF-MEMS switch in Fig. 1a. One can see the dielectric on electrode D and an air-gap between the beam and the substrate.

978-1-4577-1680-5/12/$26.00 ©2012 IEEE

Process compatibility dictates that the dielectrics on RF-MEMS devices be deposited using CVD techniques (unlike CMOS technology where very high quality SiO2 is grown over crystalline silicon). Unfortunately, chemically deposited amorphous dielectrics are identified with having high defect densities due to imperfections in chemical bonds [3]. These defects tend to capture free charges to satisfy their valences, and therefore act as charge trap centers. During the PI state, accumulation of charges in these defects over the course of operation of RF-MEMS leads to parametric degradation phenomena like CV-curve shifts and eventually stiction [4]. Device failure on account of such dielectric charging is one of the leading reliability issues in RF-MEMS [5], limiting their suitability as a viable technology.

In section II of this paper, we will quantitatively describe the physics of RF-MEMS operation by using a modeling framework that includes both beam mechanics and its electrostatic actuation. Degradation of RF-MEMS due to CV-curve shifts has traditionally been characterized by measuring shifts in actuation voltages using accelerated stress-measure-stress cycles. However, in section III, we show that this characterization scheme for RF-MEMS degradation yields pessimistic estimates of device lifetime. We will also discuss the limitations of other existing RF-MEMS degradation characterization techniques discussed in the literature. To overcome these limitations, in section IV, we propose a "non-obtrusive" non-contact measurement technique to determine RF-MEMS degradation based on electronic measurement of natural resonance frequency of the cantilever in section IV. We subsequently verify the proposed characterization technique by simulations and measurements on a packaged RF-MEMS switch. Our conclusions are summarized in section V.

II. Physics Of RF-MEMS Operation

A. Operation of RF-MEMS switches.

We have already discussed about the bi-stable operation of a RF-MEMS device. The cantilever contacts the dielectric on the drain terminal when the gate voltage (V_G) exceeds the pull-in (PI) voltage (V_{PI}), and snaps up in air when V_G drops below pull-out (PO) voltage (V_{PO}). V_{PI} and V_{PO} are the actuation voltages of the RF-MEMS switch (see Fig. 2), and their values are important for circuit design considerations. This behavior leads to a hysteretic C-V characteristic shown in Fig. 2. When the cantilever is in contact with the dielectric (with $V_G > V_{PI}$), it can be viewed as a simple metal-insulator-metal (MIM) capacitor. Like any other MIM capacitor, the voltage across the contacts injects charges into the dielectric over a period of time (Fig. 3b). Fig. 3a indicates the various electrostatic forces acting on the cantilever beam when voltage biases are applied on the three terminals.

The deflection of a solid plate of uniform thickness under transverse load is described by the Kirchhoff-Love Plate theory. Since we are modeling a cantilever beam of uniform width, we use the one-dimensional simplified version of the plate equation, also known as the Euler-Bernoulli beam equation. This equation is used to solve for the dynamic cantilever shape and is given by –

$$\rho W H \frac{\partial^2 w(y,t)}{\partial t^2} + b\frac{\partial w(y,t)}{\partial t} + \frac{EWH^3\nabla_y^4 w}{12(1-\nu^2)} = [F_e] \ . \qquad (1)$$

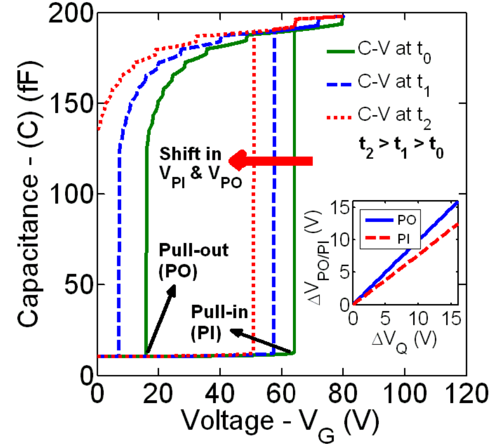

Figure 2: C-V curves of a typical cantilever RF-MEMS device with $V_B = 0$, $V_G = V_D$ and different ΔV_Q for times $t_0 = 0$, t_1 and t_2, with $t_2 > t_1 > t_0$, $\Delta V_Q(t_0) = 0$. The actuation voltages V_{PI} and V_{PO} are marked on the plot. Inset: plot of $\Delta V_{PO}$and ΔV_{PI} with varying ΔV_Q.

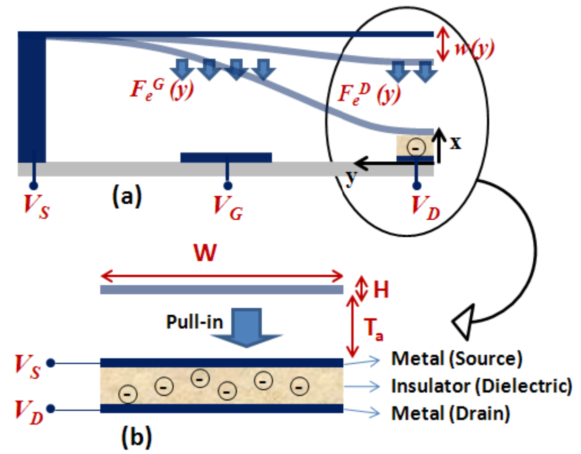

Figure 3: **(a)** Side view of the RF-MEMS switch (schematic in Fig. 1) indicating electrostatic forces acting on the cantilever membrane, and how the cantilever is pulled-in to come into contact with the dielectric on the drain electrode. **(b)** After cantilever pull-in, the voltage across the dielectric ($V_D - V_S$) injects charges into the dielectric. Some of these charges are trapped during the course of device operation.

We observe that Eq. 1 effectively represents force-balance between the electrostatic and restoring spring forces acting on the cantilever beam. Here $w(y,t)$ is the beam deflection at position y and time t (axes indicated in Fig. 3a), ρ is the mass-

density of the beam, W is the beam width (Fig. 1b), H is the beam thickness (Fig. 3b), b is the air-damping coefficient, E and ν are the Young's modulus and Poisson ratio of the beam respectively. $[F_e]$ is the downwards electrostatic force acting on the beam, and comprises of F_e^G and F_e^D, the electrostatic forces due to gate and drain biases respectively, given by –

$$F_e^G = \frac{W\epsilon_0 V_G^2}{2\left(w(y,t)\right)^2} ,$$

$$F_e^D = \frac{W\epsilon_0 \epsilon_r^2 V_D^2}{2\left(T_d + \epsilon_r w(y,t)\right)^2} .$$

Here T_d is the dielectric thickness (Fig. 1b) and ϵ_r is the relative permittivity of the dielectric.

B. Degradation and failure due to dielectric charging.

When the cantilever beam is pulled-in, it comes into contact into the dielectric on the drain. The resulting electric field across the dielectric results in charge accumulation. The effect of dielectric charging at time t is accounted for by $\Delta V_Q(t)$, which is the effective change in the drain voltage. Given the knowledge of the spatial charge density $Q(x,t)$ inside the dielectric, $\Delta V_Q(t)$ can be calculated as follows:

$$\Delta V_Q(t) = \frac{-1}{\epsilon_0 \epsilon_r} \int_0^{T_d} (T_d - x) Q(x,t) dx \ . \quad (2)$$

Details on the dynamics of trapped charge accumulation in the dielectric, and consequently the temporal evolution of $Q(x)$ and ΔV_Q have been discussed in detail in Ref. [6],[7], and not repeated here. These trapped charges modify the electrostatic force on the cantilever beam due to the drain (F_e^D) as follows:

$$F_e^D = \frac{W\epsilon_0 \epsilon_r^2 \left(V_D + \Delta V_Q(t)\right)^2}{2\left(T_d + \epsilon_r w(y,t)\right)^2} . \quad (3)$$

Eq. 1, in conjunction with the modified force expression given above in Eq. 3, is used to obtain time-dependent C-V characteristics of the cantilever RF-MEMS device under consideration for different amounts of dielectric charging, and is plotted in Fig. 2. The injected charges (represented by ΔV_Q) gradually change the electrostatic behavior of the device, leading to shifts in the C-V curves. This is, therefore, accompanied by corresponding shifts in the actuation voltages V_{PI} and V_{PO}. The device is said to have failed due to *stiction* when the cantilever cannot be pulled out even under zero applied bias, which occurs when $V_{PO} \leq 0$. The inset in Fig. 2 shows how the measured actuation voltages of the switch will change for different ΔV_Qs.

III. Traditional Characterization Techniques

A. Large-signal CV method.

Correct characterization of the temporal evolution of actuation voltages ($\Delta V_{PO}(t)$ and $\Delta V_{PI}(t)$) in RF-MEMS due to dielectric charging is important for reliability predictions. Traditionally, these quantities have been determined by accelerated testing using consecutive Stress-Measure-Stress cycles. The stress-cycle injects charges for short time periods under higher operating conditions of V_D and temperature. The measure-cycle is a C-V sweep to determine the shift in actuation voltages. In this method, the MEMS membrane comes into contact with the dielectric even during the measure-cycle, thereby disturbing the existing charges accumulated during the stress-cycle.

We simulate the aforementioned experimental characterization technique using Eq. 1 to solve for beam behavior and actuation voltages (V_{PI} and V_{PO}), and the dielectric charging model discussed in Ref. [6],[7] to obtain values for $\Delta V_Q(t)$. We compare $\Delta V_{PO}(t)$ obtained after performing both stress and measure cycles to its uncorrupted value if the C-V measure cycle could be omitted. This comparison will help us quantify the effect of the C-V measure cycle on the RF-MEMS lifetime estimates. The RF-MEMS switch is first stressed at a stress voltage greater than V_{PI} (so that the cantilever pulls-in) for a stress time t_S. The device is then subjected to a C-V sweep as a part of the measure-cycle. The stress and measure steps are repeated multiple times.

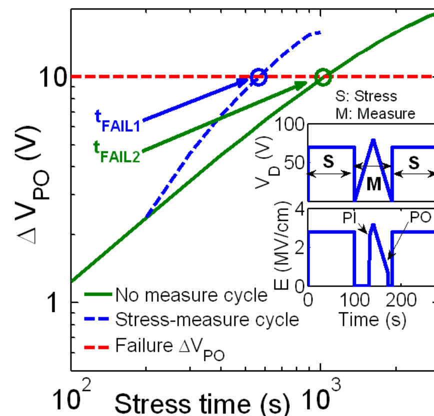

Figure 4: Simulation of a typical characterization procedure for RF-MEMS lifetime using consecutive stress-measure-stress cycles, comparing expected $\Delta V_{PO}(t)$ with (*green/solid line*) and without (*blue/dashed line*) measure step. The device is said to have failed when ΔV_{PO} exceeds an arbitrary preset value of 10V. We observe that traditional failure characterization using stress-measure-stress cycles yields pessimistic estimates of device lifetime.

In Fig. 4 we plot the shift in actuation voltages ($\Delta V_{PO}(t)$) due to dielectric charging vs. total stress time. The blue/dashed line represents $\Delta V_{PO}(t)$ due to dielectric charges accumulated

as a result of *both* the stress and measure cycles, whereas the green/solid line represents $\Delta V_{PO}(t)$ due to dielectric charges accumulated *only* during the stress cycle. We find that the actuation voltage shifts expected on the basis of the stress-cycle alone are lower than what we obtain if we perform the measure-cycle. This is because the dielectric is stressed further during the CV-sweep in the measure-cycle when cantilever is in the pulled-in state. This is demonstrated using the inset of Fig. 4, which shows a jump in the dielectric electric field during the measure-cycle when the cantilever is pulled-in. We thus find that this experimental characterization technique will yield pessimistic estimates for the device lifetime.

B. *Traditional non-contact techniques.*

The discussion above suggests that it is preferable to use a "non-obtrusive" non-contact technique during measure-cycle which does not involve cantilever pull-in. In recent literature, non-contact techniques like Kelvin Probe Force Microscopy (KPFM) [8] and optical resonance detection [9] on RF-MEMS for dielectric charge measurements have been used, but these techniques require optical/physical access to the cantilever membrane. Often in the case of pre-packaged devices, for example, this is not possible. The center-shift method [10] determines ΔV_{PO} by shifts in the C-V minima when cantilever is in PO. However, its sensitivity/accuracy for small ΔV_{PO} is unknown, since it uses curve-fitting to determine C-V minima.

IV. PROPOSED RESONANCE BASED TECHNIQUE

In this section, we propose a new characterization scheme to measure and quantify dielectric charging, and consequently determine the correct ΔV_{PO} in RF-MEMS. This method is based on detecting beam-resonances in a purely electronic manner, and calibrating the shift in resonance frequencies with respect to the amount of dielectric charging. Since this method does not involve membrane contact with the dielectric during the measure-cycle, it eliminates the limitations of using C-V measurements for lifetime characterization. Furthermore, since it is a purely electronic measurement technique, it opens up possibilities for "*in-situ*" circuit implementations and "parallel" measurements for faster technology qualification.

A. *Theory of resonance-technique*

To simulate cantilever resonance, we solve the dynamic Euler-Bernoulli beam equation (Eq. 1) using a sinusoid voltage actuation in time. The externally applied voltage has a DC shift of V_{DC}, and a small signal AC actuation voltage component V_{AC}, with angular frequency ω. We compute the small signal capacitance (C_{meas}) resulting from the cantilever oscillations as follows–

$$C_{meas} = \frac{\|I_A\|}{V_{AC}\omega} ,$$

where $\|I_A\|$ is the amplitude of the displacement current resulting due to the beam oscillation. I_A is calculated as –

$$I_A = \frac{d(CV)}{dt} = \frac{d\big(C(t)(V_{DC} + V_{AC}\sin(\omega t))\big)}{dt} .$$

The resonance frequency (F_{RES}) is obtained from the maxima in the frequency response of C_{meas} (inset - Fig. 5).

We compute the expected small signal capacitance (C_{meas}) for given voltage bias conditions over a range of frequencies (F), and extract the resonance frequency F_{RES}. F_{RES} is found to reduce with increasing V_G (Fig. 5), resulting due to a phenomena also known as the spring softening effect [10]. Additionally, for a given V_G, F_{RES} is found to reduce further with increasing trapped charges in the dielectric (increasing ΔV_Q). The change in F_{RES} (ΔF_{RES}) for a given V_G therefore reflects on ΔV_Q, and subsequently can be used as a direct indicator for the amount of dielectric charging. As seen from the inset of Fig. 2, ΔV_Q can be correlated to ΔV_{PO}, enabling us to extract the actuation voltage shifts from shifts in cantilever resonance frequencies.

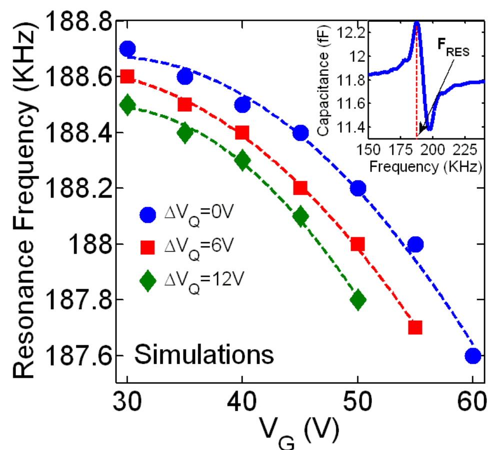

Figure 5: Simulation of shifts in resonance frequency (F_{RES}) of a cantilever based RF-MEMS device for different degrees of dielectric charging (ΔV_Q). Inset: Determining F_{RES} from the maxima of measured C-F curve.

B. *Measurement setup and procedure.*

In the previous sub-section, we discussed, theoretically, how shifts in resonance frequency can be used to obtain information about the amount of charge accumulation in the dielectric. We now validate the concept using measured data. The C-F measurements for cantilever MEMS devices to determine F_{RES} are performed on Radant MEMS ohmic switches [11]. Agilent E4980A LCR meter is used to measure C_{meas} vs. F. Keithley 4200SCS is used as source unit for V_G. The schematic of the experimental setup is shown in Fig. 6. For this switch, an external series capacitor (C_S=46pF) has been used to represent the dielectric on the drain, and an

external DC voltage bias $V_D = \Delta V_Q$ is applied to represent the effect of dielectric charging.

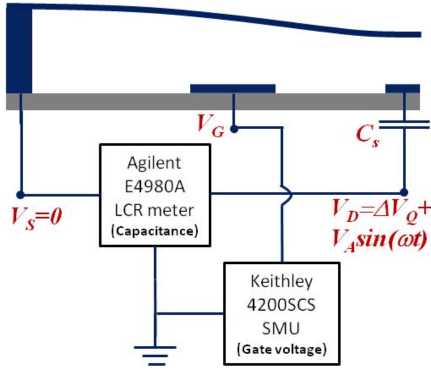

Figure 6: Schematic for the setup used for resonance measurements on RF-MEMS switches. A series capacitor C_S(=46pF) acts as a dielectric and the applied drain bias (V_D) represents the effective change in drain voltage due to dielectric charging (ΔV_Q).

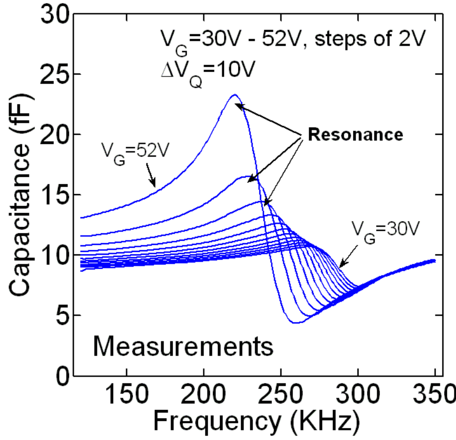

Figure 7: Results of resonance measurements done on RF-MEMS switches using the setup described in Fig. 6. C-F curves obtained for ΔV_Q=10V, by varying $V_G$between 30V-52V in steps of 2V. F_{RES} is determined form the peak capacitance point. We observe that the frequencies at the peak capacitance point decreases with increase in V_G.

Similar to the method used in simulations, we obtain the resonance frequency – F_{RES} from the maxima in the measured C_{meas}-F curves. The nature and general shape of the measured $C_{meas} - F$ characteristics are equivalent to those obtained from simulations. These curves are plotted in Fig. 7 for different V_Gs for ΔV_Q=10V. Variation of F_{RES} over a range of V_G values for different values of ΔV_Q is plotted in Fig. 8. We observe that, similar to the trends obtained from simulations, F_{RES} reduces with increasing V_G due to the spring-softening effect. Additionally, it is found to reduce further with increasing ΔV_Q for given V_G. These results therefore confirm our hypothesis that shifts in resonance frequency of the cantilever can be used as an indicator for the amount of charge accumulation in the dielectric.

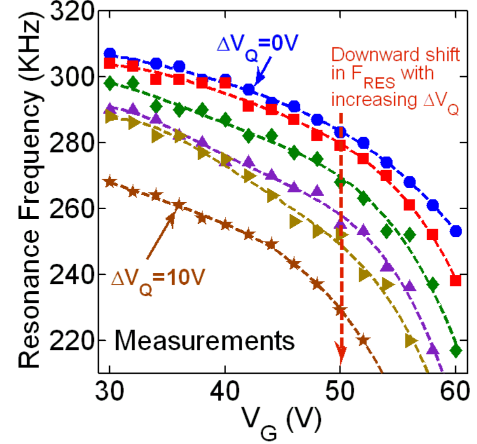

Figure 8: Plot of F_{RES} with varying V_G and ΔV_Q, similar to the simulation results plotted in Fig.4. ΔV_Q is varied between 0V and 10V in steps of 2V. The trends observed in measurements of ΔF_{RES} are the same as those expected from simulations.

C. Data analysis and interpretation.

From the results plotted in Fig. 8, we can extract the dependence of ΔF_{RES} on ΔV_Q for a given V_G (plot for V_G=50V shown in Fig. 9a). In section 2, we discussed how dielectric charge accumulation affects actuation voltages of a RF-MEMS device, and obtained the dependence of ΔV_{PO} on ΔV_Q (inset of Fig. 2, redrawn in Fig. 9b). Data in Fig. 9a and 9b can be combined by eliminating the common axis of ΔV_Q to obtain the relationship between ΔF_{RES} and ΔV_{PO} (Fig. 9c). This enables us to correlate shifts in resonance frequency to the expected shifts in actuation voltages, without really actuating the device. In Fig. 9c, we set an arbitrary value of ΔV_{PO}=10V as the failure threshold for actuation voltage shift ($\Delta V_{PO}(fail)$). The value of ΔF_{RES} at $\Delta V_{PO}(fail)$ ($\Delta F_{RES}(fail)$) is therefore the threshold for resonance frequency shift which marks the onset of device failure. This threshold value typically varies according to circuit and device design considerations.

Since ΔV_Q evolves over time due to dielectric charge injection, this effect manifests in an observed temporal evolution of ΔF_{RES}. Using the dielectric charging model described in Ref. [6],[7] in conjunction with the Euler-Bernoulli beam equation in Eq. 1, we simulate a typical expected temporal evolution of ΔF_{RES}, plotted in Fig. 9d. The device fails when $\Delta F_{RES}(fail)$ is reached, at time t_{FAIL}. Note that this failure time is the same as t_{FAIL2} in Fig. 4, which corresponds to the expected failure time without the interference of measure-cycles. Since this measurement method does not involve membrane pull-in, it will not disturb the existing dielectric charges accumulated during accelerated stress conditions, and thus giving correct lifetime estimates.

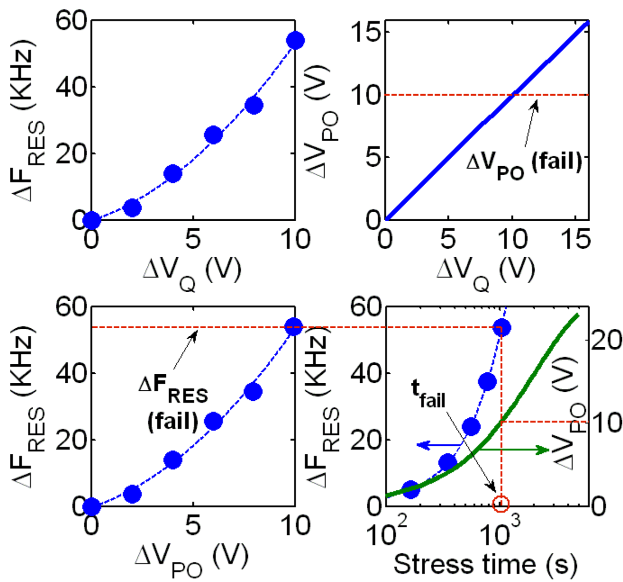

Figure 9: **(a)** Plot of ΔF_{RES} vs. ΔV_Q at $V_G = 50V$ as obtained from measurements (Fig. 8). **(b)** Plot of expected ΔV_{PO} vs. ΔV_Q as obtained from simulations (inset: Fig. 2). The failure ΔV_Q is determined when the curve crosses a threshold value of $\Delta V_{PO} = 10V$. **(c)** Experimentally observed ΔF_{RES} is mapped to ΔV_{PO} using Fig. 9(a) and Fig. 9(b). Failure ΔF_{RES} is obtained for $\Delta V_{PO} = 10V$. **(d)** Simulation of expected temporal evolution of ΔF_{RES} using Fig. 9(c) and Eq. 1, demonstrating how RF-MEMS degradation due to dielectric charging can be characterized. The device is said to have failed when ΔF_{RES} crosses the critical value of ΔF_{RES}(fail). Note that the lifetime obtained by this method is expected to be the same as t_{FAIL2} in Fig. 4.

Although resonances were detected by capacitance measurements over a frequency range in this study, a lock-in amplifier [12] can be used to obtain quick and immediate F_{RES} readouts. This gives an added advantage of the possibility of device degradation monitoring system being implemented in-situ on the chip. Furthermore, the pure electronic nature of this characterization technique enables massive large scale parallelizable measurements, which allows fast collection of data for obtaining Weibull-like distributions, implying faster and more reliable technology qualifications.

V. CONCLUSIONS

We have explained how the traditional stress-measure-stress cycle characterization for RF-MEMS degradation due to dielectric charging can yield pessimistic estimates of device lifetime. To overcome this limitation, we have proposed a "non-obtrusive" electronic scheme to detect resonance frequency of RF-MEMS membrane as an indicator of dielectric charging. This technique has been validated both by simulations and measurements. The proposed technique offers considerable improvement over existing techniques because – (1) it does not disturb existing dielectric charges deposited during stress cycles, since the measurement is done in the pulled-out state, (2) resonance detection is done by using electronic means, therefore it does not require physical/optical access to the cantilever, and consequently can be used on packaged devices, and (3) the possibility of on-chip and/or large scale parallel implementations using lock-in amplifier circuits providing in-situ monitoring capability of RF-MEMS degradation, and offering faster and more reliable technology qualification. Although the theory and characterization technique described in this work targets cantilever beam MEMS switches, the concept is geometry independent and would apply equally well to other systems.

ACKNOWLEDGEMENTS

The authors would like to acknowledge NNSA-PRISM (#DE-FC52-08NA28617) and MIT-MSD (#5710002706) centers for funding and support. They are also grateful to Prof. Peter Ye (ECE, Purdue University) for providing characterization equipment, to Andrew Kovacs (ECE, Purdue University) for providing the image of a cantilever RF-MEMS switch (Fig. 1a), and to Network for Computational Nanotechnology (NCN - #0634750-EEC) for computational resources.

REFERENCES

[1] J.J. Yao, "RF MEMS from a device perspective," *Journal of Micromechanics and Microengineering*, vol. 10, 2000, pp. R9-R38.

[2] G.M. Rebeiz and J.B. Muldavin, "RF MEMS switches and switch circuits," *Microwave Magazine, IEEE*, vol. 2, 2001, pp. 59 -71.

[3] J. Robertson and M. Powell, "Gap States in Silicon-Nitride," *Applied Physics Letters*, vol. 44, 1984, pp. 415-417.

[4] W.M. van Spengen, R. Puers, R. Mertens, and I. De Wolf, "Experimental characterization of stiction due to charging in RF MEMS," *International Electron Devices 2002 Meeting, Technical Digest*, IEEE, 2002, pp. 901-904.

[5] W.A. de Groot, J.R. Webster, D. Felnhofer, and E.P. Gusev, "Review of Device and Reliability Physics of Dielectrics in Electrostatically Driven MEMS Devices," *IEEE Transactions on Device and Materials Reliability*, vol. 9, 2009, pp. 190-202.

[6] S. Palit and M.A. Alam, "Theory of charging and charge transport in 'intermediate' thickness dielectrics and its implications for characterization and reliability," *Journal of Applied Physics (2012 - accepted)*.

[7] A. Jain, S. Palit, and M.A. Alam, "A Physics-Based Predictive Modeling Framework for Dielectric Charging and Creep in RF MEMS Capacitive Switches and Varactors," *Microelectromechanical Systems, Journal of*, vol. early-access, 2012, pp. 1 -11.

[8] U. Zaghloul, B. Bhushan, F. Coccetti, P. Pons, and R. Plana, "Kelvin probe force microscopy-based characterization techniques applied for electrostatic MEMS/NEMS devices and bare dielectric films to investigate the dielectric and substrate charging phenomena," *Journal of Vacuum Science & Technology A*, vol. 29, 2011, p. 051101.

[9] J.W. Lee, A.K. Mahapatro, D. Peroulis, and A. Raman, "Vibration-Based Monitoring and Diagnosis of Dielectric Charging in RF-MEMS Switches," *Journal of microelectromechanical systems*, vol. 19, 2010, pp. 1490-1502.

[10] R.W. Herfst, H.G.A. Huizing, P.G. Steeneken, and J. Schmitz, "Characterization of dielectric charging in RF MEMS capacitive switches," *Proceedings of the 2006 International Conference on Microelectronic Test Structures*, IEEE, 2006, pp. 133-136.

[11] "Radant MEMS," *http://www.radantmems.com*.

[12] C. Azzolini, A. Magnanini, M. Tonelli, G. Chiorboli, and C. Morandi, "Integrated lock-in amplifier for contactless interface to magnetically stimulated mechanical resonators," *Design and Technology of Integrated Systems in Nanoscale Era, 2008. DTIS 2008. 3rd International Conference on*, 2008, pp. 1 -6.